Gas Separation

International Edition: DOI: 10.1002/anie.201809884
German Edition: DOI: 10.1002/ange.201809884

Simultaneous Trapping of C_2H_2 and C_2H_6 from a Ternary Mixture of $C_2H_2/C_2H_4/C_2H_6$ in a Robust Metal–Organic Framework for the Purification of C_2H_4

Hong-Guo Hao, Yun-Feng Zhao, Di-Ming Chen, Jia-Mei Yu, Kui Tan, Shengqian Ma, Yves Chabal, Zhi-Ming Zhang, Jian-Min Dou, Zi-Hui Xiao, Gregory Day, Hong-Cai Zhou,* and Tong-Bu Lu**

Abstract: *The removal of C_2H_2 and C_2H_6 from C_2H_4 streams is of great significance for feedstock purification to produce polyethylene and other commodity chemicals but the simultaneous adsorption of C_2H_6 and C_2H_2 over C_2H_4 from a ternary mixture has never been realized. Herein, a robust metal–organic framework, TJT-100, was designed and synthesized, which demonstrates remarkably selective adsorption of C_2H_2 and C_2H_6 over C_2H_4. Breakthrough experiments show that TJT-100 can be used as an adsorbent for high-performance purification of C_2H_4 from a ternary mixture of $C_2H_2/C_2H_4/C_2H_6$ (0.5:99:0.5) to afford a C_2H_4 purity greater than 99.997 %, beyond that required for ethylene polymerization. Computational studies reveal that the uncoordinated carboxylate oxygen atoms and coordinated water molecules pointing towards the pore can trap C_2H_2 and C_2H_6 through the formation of multiple C–H···O electrostatic interactions, while the corresponding C_2H_4–framework interaction is unfavorable.*

Light hydrocarbons, such as ethane, ethylene, and acetylene, are the most widely used feedstock molecules in the petrochemical industry.[1,2] In particular, ethylene, one of the most essential chemical feedstocks in the world, is widely utilized in the production of multiple commodity chemicals, including polyethylene. Within the petrochemical industry, ethylene is mainly obtained by steam cracking of naphtha and the dehydrogenation of ethane.[3] During these processes, two major impurities are acetylene and ethane. Acetylene is a known poison for many common ethylene polymerization catalysts, reacting with catalytic metals to form acetylides, which have been known to cause gas flow blockages and explosions.[3] The presence of high levels of C_2H_6, on the other hand, can result in longer reactor residence times and decreases the production output per unit time. In addition, non-reactive C_2H_6 will often end up leaving the process after off-gassing from the finished polymer, which can be a source of health and safety concerns. The separation of a C_2H_4/C_2H_6 mixture is perceived as one of the most challenging yet important industrial processes, owing to the similar molecular sizes and volatilities of C_2H_4 and C_2H_6. At present, the most commonly used method for the industrial separation of C_2H_4/C_2H_6 mixture is high-pressure cryogenic distillation, an extremely costly and energy-intensive process.[4] Up to now, new approaches for effective C_2H_2/C_2H_4 or C_2H_6/C_2H_4 separation have focused on membrane separations, organic solvent sorbent based separations, and metall–organic framework (MOF) adsorbent based separations.

In the past decades, MOFs have emerged as a new type of advanced functional porous materials for the separation of C_2H_2/C_2H_4 or C_2H_6/C_2H_4 mixtures.[5–13] Up to now, many MOFs have shown outstanding performance in the separation of C_2H_2/C_2H_4.[5,9] For C_2H_4/C_2H_6, it is well known that unsaturated C_2H_4 can easily bind to the open metal sites, leading to highly selective uptake of C_2H_4 over C_2H_6.[10] However, in such a process, the inert C_2H_6 is recovered first, with C_2H_4 only being obtained through heating or by purging with an inert gas. As such, it is difficult to obtain the desired C_2H_4 product with high purity if C_2H_6 is utilized as the mobile phase. The examination of adsorbents with highly selective adsorption of C_2H_6 from a C_2H_4/C_2H_6 mixture could reduce the energy consumption of these separation processes affording high-purity C_2H_4. Until now, only a few low-polarity or hydrophobic MOFs have been reported to possess such an unusual adsorption behavior.[4,11,12] To the best of our knowl-

[*] Prof. Y. F. Zhao, Prof. Z. Zhang, Dr. Z. H. Xiao, Prof. T. B. Lu
Institute for New Energy Materials and Low Carbon Technologies
School of Materials Science and Engineering
Tianjin University of Technology
Tianjin 300384 (China)
E-mail: zmzhang@email.tjut.edu.cn
lutongbu@tjut.edu.cn

Dr. H. G. Hao, Prof. J. M. Dou
School of Chemistry and Chemical Engineering
Liaocheng University, Liaocheng 252059 (China)

Dr. D. M. Chen
Zhengzhou University of Light Industry
Zhengzhou 450002 (China)

J. M. Yu, G. Day, Prof. H. C. Zhou
Department of Chemistry, Texas A&M University
College Station, TX 77843-3255 (USA)
E-mail: zhou@chem.tamu.edu

Dr. K. Tan, Prof. Y. Chabal
Department of Materials Science & Engineering
University of Texas at Dallas
Richardson, TX 75080 (USA)

Prof. S. Ma
Department of Chemistry, University of South Florida
4202 E. Fowler Avenue, Tampa, FL 33620 (USA)

Supporting information and the ORCID identification number(s) for the author(s) of this article can be found under: https://doi.org/10.1002/anie.201809884.

edge, MOFs that can simultaneously and selectively absorb C_2H_6 and C_2H_2 over C_2H_4 from a ternary mixture of C_2H_2/C_2H_4/C_2H_6 have never been described.

Herein, we report such a rare example, a stable porous MOF, $(Me_2NH_2)[Co_3(DCPN)_2(\mu_3\text{-}OH)(H_2O)]\cdot 11\,H_2O$ (TJT-100, DCPN = 5-(3′,5′-dicarboxylphenyl)nicotinate). The proper positioning of uncoordinated carboxylate oxygen atoms and coordinated water molecules on the microporous pore surface can simultaneously trap C_2H_2 and C_2H_6 through the formation of weak electrostatic interactions with the C–H bonds of C_2H_6 and C_2H_2, a situation that does not appear to occur with C_2H_4. This leads to the efficient purification of C_2H_4 (purity > 99.997 %) from a ternary mixture of C_2H_2/C_2H_4/C_2H_6 with this MOF as an adsorbent in a single breakthrough operation at room temperature.

TJT-100 crystallizes in the orthorhombic space group *Pbca*, and exhibits a three-dimensional (3D) porous structure with a high density of carboxylate oxygen atoms on the surfaces of the 1D pores (Figure 1 a; see also the Supporting Information, Figures S1–S3). In one asymmetric unit, there are three crystallographically independent Co^{2+} ions that form a trinuclear $Co_3(\mu_3\text{-}OH)(O_2C)_4$ ({Co_3}) cluster as a secondary building unit (SBU; Figure 1 b). In {Co_3} SBU, both Co1 and Co3 adopt a six-coordinated octahedral configuration. As shown in Figure 1 b, Co1 is coordinated by four carboxylate oxygen atoms, one μ_3-OH, and one pyridyl N atom, and Co3 is coordinated by four carboxylate oxygen atoms, one coordinated water molecule, and one μ_3-OH oxygen atom. Co2 is five-coordinated with three carboxylate O atoms, one pyridyl N atom, and one μ_3-OH, showing a distorted trigonal-bipyramidal configuration. It is noteworthy that there are two uncoordinated carboxylate oxygen atoms around the Co1 and Co3 centers, which might be able to interact with guest molecules through electrostatic interactions. Furthermore, the {Co_3} SBUs are linked together by DCPN ligands, generating an anionic skeleton with 1D pores running along the *b* axis (ca. 8.7×11.6 Å^2). The negative charge of the host framework is balanced by $Me_2NH_2^+$ cations (Figure S2). The phase purity of the bulk product was confirmed by comparison of its experimental and simulated PXRD patterns (Figure S4 a).

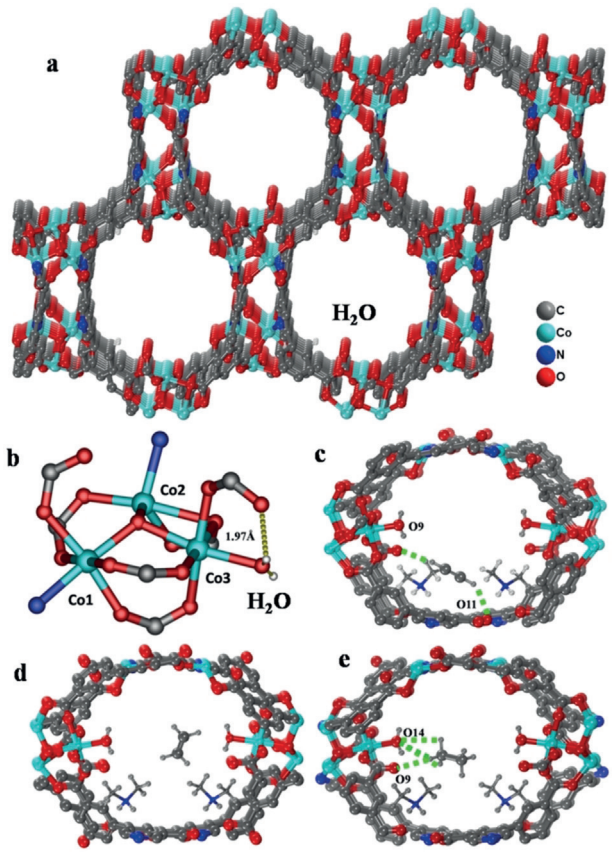

Figure 1. a) The structure of TJT-100 viewed along the *b* axis ($Me_2NH_2^+$ and guest water molecules are omitted for clarity). b) Trinuclear {Co_3} SBUs in TJT-100. Preferential adsorption sites for c) C_2H_6, d) C_2H_4, and e) C_2H_2 in TJT-100 as revealed by computational simulations.

Remarkably, TJT-100 exhibits high thermal and chemical stability (Figures S4–S7), which prompted us to investigate its gas adsorption and separation properties.[14–17] To examine the gas adsorption capacity, the N_2 adsorption isotherm of activated TJT-100 was investigated at 77 K (Figure 2 a). A

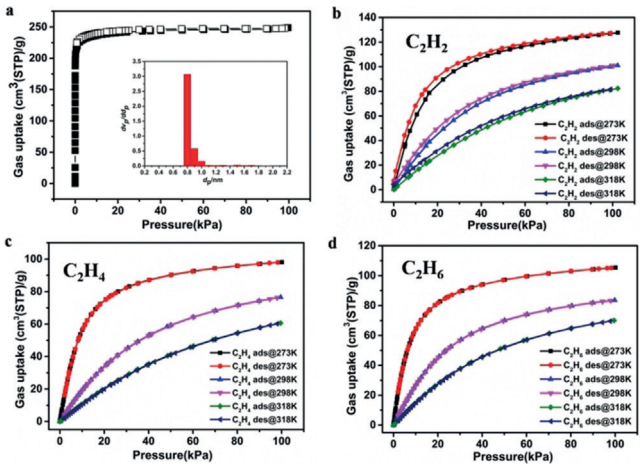

Figure 2. a) N_2 sorption and desorption isotherms at 77 K for activated TJT-100 (inset: pore-size distribution). Adsorption and desorption isotherms of activated TJT-100 for b) C_2H_2, c) C_2H_4, and d) C_2H_6 at 273, 298, and 318 K, respectively.

typical type I microporous isotherm was generated, confirming the permanent porosity of TJT-100, with a Brunauer–Emmett–Teller (BET) surface area of 890 $m^2 g^{-1}$ (Langmuir surface area of 1077 $m^2 g^{-1}$) and a mean pore size of approximately 8.0 Å. Measurements of the C_2H_2, C_2H_4, and C_2H_6 gas adsorption capacities of activated TJT-100 were also performed. Single-component adsorption isotherms for C_2H_2, C_2H_4, and C_2H_6 up to 1 atm were measured at 273, 298, and 318 K, respectively (Figure 2 and Tables S2–S5). As expected, the amount of adsorbed gas in activated TJT-100 decreased with increasing temperature. In addition, the adsorption capacity of activated TJT-100 is lower for C_2H_4 than for C_2H_2 and C_2H_6 at all analyzed temperatures (Figure 2), which contrasts those of previously reported MOFs, with adsorption capacities in the order of $C_2H_2 > C_2H_4 > C_2H_6$ (Table S2). The isosteric heats of adsorption (Q_{st}) were calculated to evaluate

the binding energies between the C_2 gases and the TJT-100 framework. As shown in Figure 3a and Table S2, the order of Q_{st} values at zero coverage is C_2H_2 (31 kJ mol^{-1}) > C_2H_6 (29 kJ mol^{-1}) > C_2H_4 (25 kJ mol^{-1}), which is consistent with

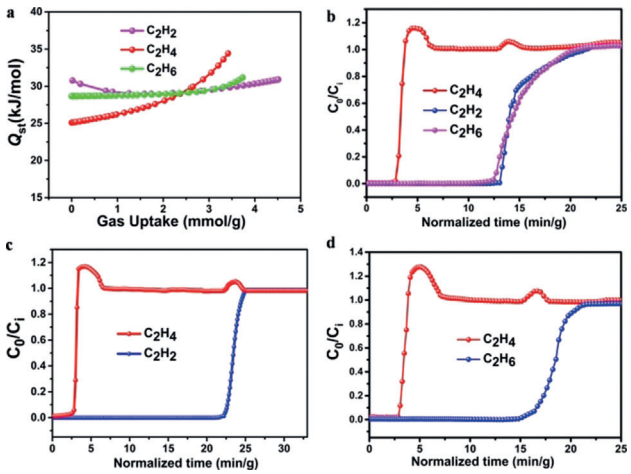

Figure 3. a) The calculated Q_{st} values of activated TJT-100 for C_2H_6, C_2H_4, and C_2H_2 at 298 K. Breakthrough curves of activated TJT-100 for b) $C_2H_6/C_2H_2/C_2H_4$ (0.5:0.5:99), c) C_2H_2/C_2H_4 (1:99), and d) C_2H_6/C_2H_4 (1:99) measured at 298 K and 1 bar; C_i and C_o are the concentrations of the inlet and outlet gases, respectively.

the uptake amounts determined from the adsorption isotherms. Typically, the Q_{st} values for C_2H_2, C_2H_4, and C_2H_6 decrease in the order of $C_2H_2 \geq C_2H_4 > C_2H_6$[2] in previously reported MOFs (Table S2). The higher C_2H_6 Q_{st} value of activated TJT-100 indicates that the positioning of the functional groups within this framework enables efficient adsorption of the inert C_2H_6 molecule. Single-component isotherms for 1:99 C_2H_2/C_2H_4 and C_2H_6/C_2H_4 mixtures at 273 and 298 K were fitted by ideal adsorbed solution theory (IAST).[18] As shown in Figure S10, the adsorption selectivities for C_2H_2/C_2H_4 and C_2H_6/C_2H_4 at a pressure of 1 atm and 298 K were calculated to be 1.8 and 1.2, respectively, indicating the feasibility of using activated TJT-100 for practical applications in the separation of C_2H_4 from C_2H_2 and C_2H_6.[2,4,19]

To evaluate the separation potential of activated TJT-100 for C_2H_2/C_2H_4 and C_2H_6/C_2H_4 gas mixtures, key experiments were carried out with binary mixtures of C_2H_2/C_2H_4 (1:99 v/v) and C_2H_6/C_2H_4 (1:99 v/v), which are typical compositions of industrial mixtures. As shown in Figure 3b,c, highly efficient separation of C_2H_4 from a 1:99 gas mixture of C_2H_2/C_2H_4 was achieved by passing the mixture over a packed column of activated TJT-100. It can be observed that C_2H_4 achieves a breakthrough first, with no evidence of C_2H_2 or C_2H_6 flow before its breakthrough point. Thus the concentrations of C_2H_2 and C_2H_6 in the outlet gas are both below 3 ppm (lower than the detection limit of the GC, 0.003%), enabling the collection of ethylene with an extremely high purity greater than 99.997% after only a single-breakthrough operation (Figures S11 and S12). The actual gas separation selectivities for 1:99 v/v C_2H_2/C_2H_4 and 1:99 v/v C_2H_6/C_2H_4 gas mixtures were 8.5 and 5.75, respectively, as determined by dual-component breakthrough experiments. Breakthrough experiments were also conducted using a ternary mixture of $C_2H_2/C_2H_6/C_2H_4$ (0.5:0.5:99 v/v/v) with activated TJT-100 as the adsorbent (Figure 3d). Again, only a single adsorption–desorption cycle was required to achieve an ethylene purity of greater than 99.997% (Figure S13). This purity is much higher than that required for a typical ethylene polymerization reactor.[2] These results suggest TJT-100 as a high-performance adsorbent for the potential purification of ternary mixtures of C_2 hydrocarbons into high-purity ethylene for use in the petrochemical industry.

The investigation of gas–framework interactions is significant for understanding the above unique adsorption behavior. One of the most effective methods is to determine the gas binding sites by single-crystal diffraction.[20,21] However, single-crystal data of activated TJT-100 with absorbed C_2 molecules could not be obtained even after several attempts. Therefore, grand canonical Monte Carlo (GCMC) simulations, which have been widely used to understand the nature of gas adsorption sites within such frameworks,[22–25] were used to study the adsorption properties of C_2 gases on activated TJT-100. The GCMC results gave simulated C_2H_2, C_2H_4, and C_2H_6 uptakes of 105, 80, and 86 cm^3 g^{-1}, respectively, for activated TJT-100 at 298 K and 1 bar; these values are close to the experimental results, validating the use of the CMC method for the TJT-100 system. The calculated potential fields for these gases were shown by the way of slice (Figures S14–S16). As shown in Figure S14, the highest potential values for C_2H_2 are near uncoordinated carboxylate oxygen atoms, $Me_2NH_2^+$ cations, and phenyl rings of the ligand. The slice of the calculated potential field for C_2H_6 shows that the highest potential values are located around the coordinated water molecules, uncoordinated carboxylate oxygen atoms, and $Me_2NH_2^+$ cations (Figure S15).[21] For C_2H_4, the slice suggests no obvious strong affinity between the C_2H_4 molecules and the framework (Figure S16). These results are in good agreement with the breakthrough experiments that show a low affinity of C_2H_4 towards activated TJT-100.

Electrostatic interactions between donor oxygen atoms and gas molecules are known to play important roles in the separation of light hydrocarbons by MOFs.[26] In most cases, C–H···O interactions were identified with C···O distances in the range of 3.2 < C···O < 4.0 Å.[27,28] GCMC calculations revealed that C_2H_2 molecules are bound to two uncoordinated carboxyl oxygen atoms, C–H···O9 (H···O9 2.612 Å) and C–H···O11 (H···O11 2.996 Å), through hydrogen-bonding interactions (Figures 1e and 4). In addition, C_2H_2 molecules are close to $Me_2NH_2^+$ cations and DCPN linkers in the framework of TJT-100, resulting in beneficial intermolecular van der Waals interactions (C···C distances ranging from 3.342 to 4.133 Å; Figure 4a). The high uptake of C_2H_6 in activated TJT-100 can be attributed to the existence of a large number of weak interactions between the anionic oxygen atoms and the slightly polarizable C–H bonds of C_2H_6. As shown in Figures 1c and 4d, an ethane molecule can form four interactions with the uncoordinated carboxylate oxygen atoms and coordinated water molecules through its polarizable C–H bonds. These interactions are aided by the

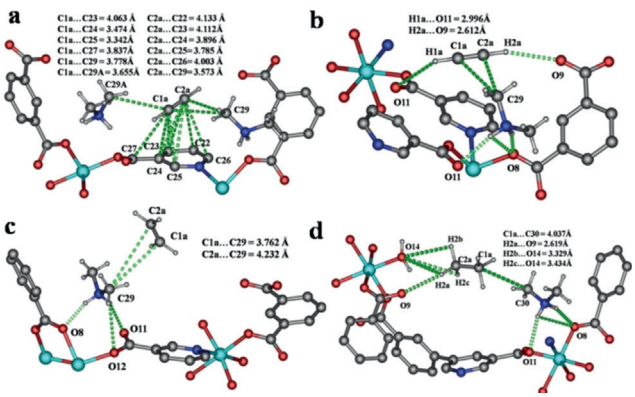

Figure 4. Results of the GCMC simulations, showing the preferential adsorption sites for a, b) C_2H_2, c) C_2H_4, and d) C_2H_6 in activated TJT-100.

polarization provided by the $Me_2NH_2^+$ cations (Figure 4 d). For C_2H_4, only weak van der Waal interactions between C_2H_4 molecules and $Me_2NH_2^+$ cations were observed (Figures 1 d and 4 c). Owing to the shorter C–C and C–H bond lengths of C_2H_4 compared to those of C_2H_6, the C–H bonds in C_2H_4 cannot be polarized enough by $Me_2NH_2^+$ to enforce a C–H···O interaction. Because of this, C_2H_4 has the lowest framework affinity amongst the three gases. All of the above results reveal an unusual affinity of TJT-100 towards inert C_2H_6 instead of unsaturated C_2H_4, giving an affinity order of $C_2H_2 > C_2H_6 > C_2H_4$. This hierarchy also agrees with the results of the breakthrough experiments, which achieved a high separation selectivity of C_2H_4 from a ternary mixture of $C_2H_2/C_2H_4/C_2H_6$ at room temperature. To further confirm the interactions between the C_2 molecules and the framework, in situ IR measurements of C_2 adsorption at room temperature were conducted on TJT-100, which confirmed the existence of stronger hydrogen-bonding interactions between C_2H_2/C_2H_6 and the uncoordinated carboxylate oxygen atoms of the framework, compared to those between C_2H_4 and TJT-100, and the existence of weak van der Waals interactions between C_2H_2 molecules and the phenyl rings of the ligands (Figures S17 and S18).

In conclusion, we have synthesized a new porous MOF, TJT-100, with high thermal and acid/base stability. This framework possesses a relatively high uptake capacity of C_2H_6, C_2H_4, and C_2H_2, and shows unique selective adsorption of C_2H_6 and C_2H_2 over C_2H_4 from a ternary mixture of $C_2H_2/C_2H_6/C_2H_4$ (0.5:0.5:99 v/v/v), achieving a C_2H_4 purity greater than 99.997 % by a single-breakthrough operation. This was mostly attributed the existence of a high density of uncoordinated carboxylate oxygen atoms and coordinated water molecules on the surfaces of the pores, which enables the capture of C_2H_6 and C_2H_2 molecules through multiple electrostatic interactions. $Me_2NH_2^+$ also plays an important role in polarizing C_2H_6 for the high affinity of TJT-100 toward C_2H_6 by forcing C–H···O interactions. This work not only reports a new stable material for potentially producing very pure C_2H_4 from a ternary mixture of $C_2H_2/C_2H_4/C_2H_6$, but also provides insight for exploring the effect of functional oxygen atoms on the separation of C_2 species in MOFs.

Acknowledgements

This work was supported by National Key R&D Program of China (2017YFA0700104), the National Natural Science Foundation of China (21401095, 21722104, 2167103, 21790052, 21331007), and the 111 Project of China (No. D17003); it was also partially funded by the Robert A. Welch Foundation through a Welch Endowed Chair to H.C.Z. (A-0030).

Conflict of interest

The authors declare no conflict of interest.

Keywords: electrostatic interactions · gas separation · light hydrocarbons · metal–organic frameworks · selective adsorption

How to cite: *Angew. Chem. Int. Ed.* **2018**, *57*, 16067–16071
Angew. Chem. **2018**, *130*, 16299–16303

[1] Z. R. Herm, B. M. Wiers, J. A. Mason, J. M. Baten, M. R. Hudson, P. Zajdel, C. M. Brown, N. Masciocchi, R. Krishna, J. R. Long, *Science* **2013**, *340*, 960–965.
[2] Y. B. He, K. Rajamani, B. L. Chen, *Energy Environ. Sci.* **2012**, *5*, 9107–9120.
[3] Z. Bao, D. Xie, G. Chang, H. Wu, L. Li, W. Zhou, H. Wang, Z. Zhang, H. Xing, Q. Yang, M. J. Zaworotko, Q. Ren, L. B. Chen, *J. Am. Chem. Soc.* **2018**, *140*, 4596–4603.
[4] P. Q. Liao, W. X. Zhang, J. P. Zhang, X. M. Chen, *Nat. Commun.* **2015**, *6*, 8697.
[5] Y. Peng, T. Pham, P. Li, T. Wang, Y. Chen, K. Chen, K. A. Forrest, B. Space, P. Cheng, M. J. Zaworotko, Z. Zhang, *Angew. Chem. Int. Ed.* **2018**, *57*, 10971–10975; *Angew. Chem.* **2018**, *130*, 11137–11141.
[6] C. Gücüyener, J. v. d. Bergh, J. Gascon, F. Kapteijn, *J. Am. Chem. Soc.* **2010**, *132*, 17704.
[7] P. Nugent, Y. Belmabkhout, S. D. Burd, A. J. Cairns, R. Luebke, K. Forrest, T. Pham, S. Ma, B. Space, L. Wojtas, M. Eddaoudi, M. J. Zaworotko, *Nature* **2013**, *495*, 80.
[8] S. R. Venna, J. B. Jasinski, M. A. Carreon, *J. Am. Chem. Soc.* **2010**, *132*, 18030–18033.
[9] X. Cui, K. Chen, H. Xing, Q. Yang, R. Krishna, Z. Bao, H. Wu, W. Zhou, X. Dong, Y. Han, B. Li, Q. Ren, M. J. Zaworotko, B. Chen, *Science* **2016**, *353*, 141.
[10] E. D. Bloch, W. L. Queen, R. Krishna, J. M. Zadrozny, C. M. Brown, J. R. Long, *Science* **2012**, *335*, 1606–1610.
[11] C. Gücüyener, J. van den Bergh, J. Gascon, F. Kapteijn, *J. Am. Chem. Soc.* **2010**, *132*, 17704–17706.
[12] J. T. Hupp, K. R. Poeppelmeier, *Science* **2005**, *309*, 2040–2042.
[13] S. Yang, A. J. R. Cuesta, R. Newby, V. G. Sakai, P. Manuel, S. K. Callear, S. I. Campbell, C. C. Tang, M. Schröder, *Nat. Chem.* **2015**, *7*, 121–129.
[14] Z. R. Herm, E. D. Bloch, J. R. Long, *Chem. Mater.* **2014**, *26*, 323.
[15] K. Wang, X.-L. Lv, D. Feng, J. Li, S. Chen, J. Sun, L. Song, Y. Xie, J.-R. Li, H.-C. Zhou, *J. Am. Chem. Soc.* **2016**, *138*, 914.
[16] L. F Yang, X. L. Cui, Z. Q. Zhang, Q. W. Yang, Z. B. Bao, Q. L. Ren, H. B. Xing, *Angew. Chem. Int. Ed.* **2018**, *57*, 13145; *Angew. Chem.* **2018**, *130*, 13329.
[17] R.-B. Lin, H. Wu, L. Li, X.-L. Tang, Z. Li, J. Gao, H. Cui, W. Zhou, B. Chen, *J. Am. Chem. Soc.* **2018**, *140*, 12940–12946.
[18] A. L. Myers, J. M. Prausnitz, *AIChE J.* **1965**, *11*, 121–130.

[19] H. Wen, B. Li, H. Wang, C. Wu, K. Alfooty, R. Krishnad, B. Chen, *Chem. Commun.* **2015**, *51*, 5610 – 5613.
[20] Y. Kubota, M. Takata, R. Matsuda, R. Kitaura, S. Kitagawa, T. C. Kobayashi, *Angew. Chem. Int. Ed.* **2006**, *45*, 4932 – 4936; *Angew. Chem.* **2006**, *118*, 5054 – 5058.
[21] S. B. Jang, M. S. Jeong, Y. Kim, *Zeolites* **1997**, *19*, 228 – 237.
[22] M. Fischer, F. Hoffmann, M. Froba, *ChemPhysChem* **2010**, *11*, 2220 – 2229.
[23] H. C. Guo, F. Shi, Z. F. Ma, X. Q. Liu, *Mol. Simul.* **2014**, *40*, 349 – 360.
[24] S. Xiang, W. Zhou, J. M. Gallegos, Y. Liu, B. Chen, *J. Am. Chem. Soc.* **2009**, *131*, 12415 – 12419.
[25] J. Pang, F. Jiang, M. Wu, C. Liu, K. Su, W. Lu, D. Yuan, M. Hong, *Nat. Chem.* **2015**, *6*, 7575.
[26] M. Chen, S. Chen, W. Chen, B. E. G. Lucier, Y. Zhang, A. Zheng, Y. Huang, *Chem. Mater.* **2018**, *30*, 3613 – 3617.
[27] G. R. Desiraju, *Acc. Chem. Res.* **1996**, *29*, 441.
[28] J. W. Steed, J. L. Atwood, *Supramolecular Chemistry*, Wiley, Chichester, **2000**, p. 26.

Manuscript received: August 31, 2018
Revised manuscript received: October 6, 2018
Accepted manuscript online: October 19, 2018
Version of record online: November 11, 2018

